

Design Analysis And Efficient Control Of Quasi-Z-Source Cascaded Multi Level Inverter For Grid Connected PV Panels

Mrs. S.Gayathri¹ , Mrs.M.Divya Charitha,² , Mr.G.Devadas³
CMRCET, JNTUH, Hyderabad
CMRCET, JNTUH, Hyderabad
CMRCET, JNTUH, Hyderabad

ABSTRACT:-*The quasi-Z source cascaded multilevel inverter presents remarkable advantages in application to photovoltaic (PV) system. Each PV panel is connected to a quasi-Z-source H-bridge inverter to form a power generation module. The paper proposes design analysis and efficient closed loop control for quasi- Z-source cascaded multilevel inverter based PV system. The distributed maximum power point tracking (MPPT) for all PV modules produce balanced dc-link peak voltage. A novel space vector modulation for the integration of shoot through states synthesize a stepped output voltage waveform of quasi-Z-source inverters. The closed loop control voltage ensures a high quality waveform to the grid. Simulation of cascaded multilevel quasi-Z-source inverter for PV system is carried out to verify the results of the above proposed concepts using MATLAB/Simulink.*

Key Words:-*Cascaded Multilevel Inverter (CMI), Photovoltaic system (PV), Space Vector Modulation (SVM).*

I. INTRODUCTION

A recent development in the study of photovoltaic power generation emerges as they directly convert the solar radiation into electrical energy without affecting the environment. But due to the effect of irradiation and temperature, fluctuation of solar power, is inconsistent with the desired stable power injected to the grid. To exploit the maximum power from the PV panels and feeding those into the grids at unity power factor become the most important.

The H-bridge module lacks the boost function so that the inverter KVA rating has to be increased twice that of the PV voltage range. Different PV panel output voltages result in imbalanced dc-link voltages. These result in high complexity of the system control and cost but also decrease the efficiency.

Recently, the quasi-Z-source cascade multilevel inverter (qZS-CMI)-based PV systems were projected. They possess the advantages of both traditional CMI and Z-source topologies. For example, the qZS-CMI: 1) shows modular topology that each inverter has the same circuit topology, control structure and modulation. 2) has high-quality staircase output voltage waveforms with lower harmonic distortions, and reduces/eliminates output filter requirements for the compliance of grid harmonic standards; 3) requires power semiconductors with a lower rating, and greatly saves the costs; 4) most important of all, has independent dc-link voltage compensation with the special voltage step-up/down function in a single-stage power conversion of quasi-Z-source network, which allows an independent control of the power delivery with high reliability and 5) can fulfill the distributed MPPT [5], [6].

In order to properly operate the qZS-CMI, the power injection, and the independent control of dc-link voltages, space vector modulation /pulse width modulation are necessary.

The main objective of this paper includes: The distributed MPPT to ensure the maximum power extraction from each PV array. The power injection to the grid at unity power factor with low harmonic distortion. The constant dc-link peak voltage for all qZS-HBI modules.

This paper is organized as follows. An overview of the whole system is presented in Section II. Section III addresses the system modelling and control. Section IV proposed multilevel svm for qZS-CMI. The proposed strategy is verified by simulation results in Section V. Finally, a conclusion is given in Section VI.

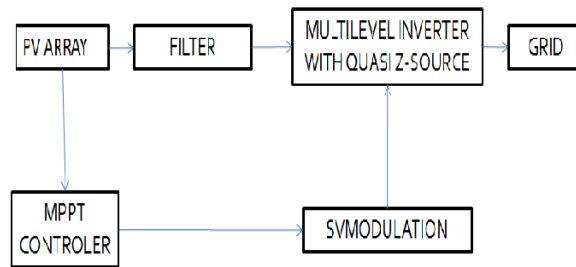


Fig 1. Block diagram of qZS-CMI based grid tie PV power system.

II qZS-CMI BASED GRID TIE PV POWER SYSTEM

A. PV Array with MPPT control:

Fig.1 shows the block diagram of qZS-CMI-based grid-tie PV power system. The individual PV power source is an array composed of identical PV panels in parallel and series. Each cell is fed by an independent PV panel. The power of the PV module varies depending on the insolation and load (operating point). So it is necessary to operate the PV at its maximum power point. Short-circuit current is directly proportional to the insolation. The solar cell operates in two regions, that is, constant voltage and constant current region. So it is essential to operate PV module at MPP always.

MPPT is a two-step procedure. First step is to plot ‘voltage’ Vs ‘power’ graph of the cell. Power is calculated by multiplying voltage across the cell with corresponding current through the cell. From the plot, maximum power point is located and corresponding voltage is noted. The second step is to go to the V-I characteristics of the cell and locate the current corresponding to the voltage at maximum power point. This current is called the current at maximum power point.

$$R_{mp} = \frac{V_{mp}}{I_{mp}}$$

DC-to-DC converter is used to balance between load and cell. The input resistance (R_{in}) depends on the load resistance and the duty cycle of converters. To the PV cell/module, the converter acts as a load and if R_{in} of the converter lies on the V_{mp} - I_{mp} point, a system that automatically sets the duty cycle D value to duty cycle for MPP D_{mp} such that maximum power can be transferred to the load. This is called Maximum Power Point Tracking or MPPT. Here Perturb & Observe (P&O) is used to obtain MPP from the PV array. The P & O algorithm states that when the operating voltage of the PV panel is perturbed by a small increment, if the resulting change in power ΔP is positive, then we are going in the direction of MPP and we keep on perturbing in the same direction. If ΔP is negative, we are going away from the direction of MPP and the sign of perturbation supplied has to be changed. Thus Maximum power can be exploited for the PV array connected to the qZS-CMI.

B. qZS-CMI:

As stated before quasi Z-source inverter is preferred for PV applications as it can buck or boost up the input voltages without changing the converter topology. qZSI draws a continuous constant dc current from the source, which makes the system well suited for PV –PCS. The rating of the components are greatly reduced. The total output voltage of the inverter is a series summation of qZS-HBI cell voltages.

The qZS-CMI combines the qZS network into each HBI module. When the qZS-HBI is in non-shoot-through states, it will work as a traditional HBI. There are

$$V_{DCK} = V_{PVk} \left[\frac{1}{1-2D_k} \right] V_{HK} = S_k \cdot V_{DCK} \quad (1)$$

while in shoot-through states, the qZS-HBI module does not contribute voltage. There are

$$V_{HK}=0 \quad V_{DCK}=0 \quad \dots \dots (2)$$

For the qZS-CMI, the synthesized voltage is

$$V_H = \sum_{k=1}^n V_{Hk} = \sum_{k=1}^n S_k \cdot V_{DCK} \dots (3)$$

where V_{PVk} is the output voltage of the k^{th} PV array, V_{DCK} is the dc-link voltage of the k^{th} qZS-HBI module; D_k represent the shoot-through duty ratio of the k^{th} qZS-HBI; V_{HK} is the output voltage of the k^{th} module, and $S_k \in \{-1, 0, 1\}$ is the switching function of the k^{th} qZS-HBI.

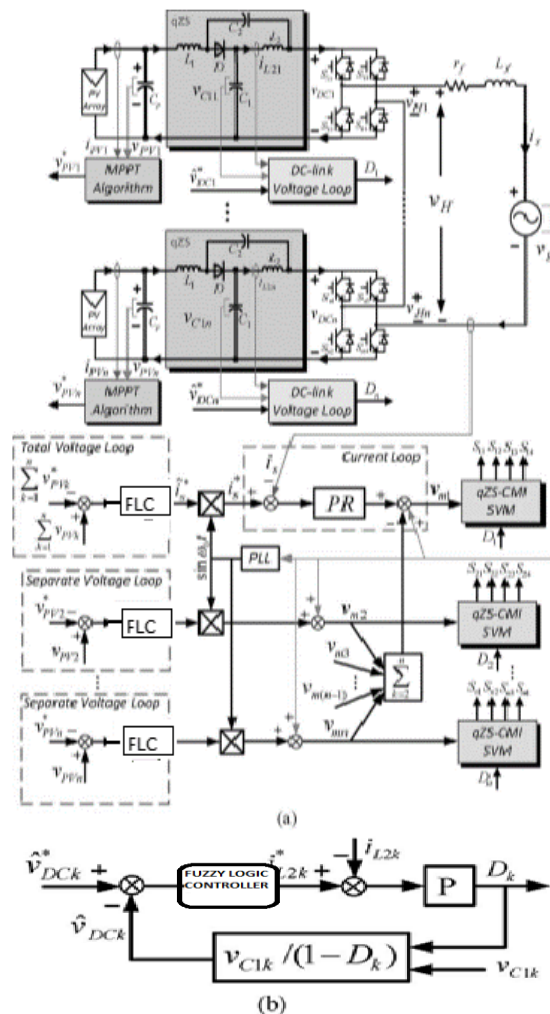
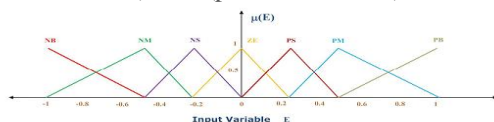


Fig 2. qZS-CMI based grid –tie PV power system with DC-link peak voltage control.

C.FUZZY LOGIC CONTROLLER:

The control scheme consists of a Fuzzy controller, a limiter, and a three phase sine wave generator for the generation of reference currents and switching signals. The peak value of the reference current is estimated by regulating the DC link voltage. The actual capacitor voltage is compared with a set reference value. The error signal is then processed through a Fuzzy controller [7], which contributes to the zero steady error in tracking the reference current signal. A fuzzy controller converts a linguistic control strategy into an automatic control strategy, and fuzzy rules are constructed either by expert experience or with a knowledge database. Firstly, the input Error ‘E’ and the change in Error ‘ ΔE ’ have been placed with the angular velocity to be used as the input variables of the fuzzy logic controller. Then the output variable of the fuzzy logic controller is presented by the control current I_{max} . To convert these numerical variables into linguistic variables, the following seven fuzzy levels or sets are chosen: NB (negative big), NM (negative medium), NS (negative small), ZE (zero), PS (positive small), PM (positive medium), and PB (positive big) as shown in below fig



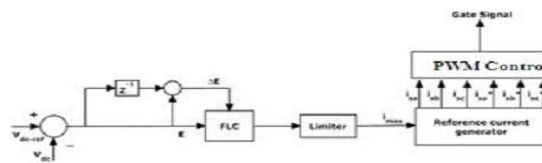


Fig 3. Block diagram for a fuzzy logic controller.

A fuzzy inference system (or fuzzy system) basically consists of a formulation of the mapping from a given input set to an output set using fuzzy logic. This mapping process provides the basis from which the inference or conclusion can be made. A fuzzy inference process consists of the following steps: 1) Fuzzification of input variables. 2) Application of fuzzy operator (AND, OR, NOT) in the IF (antecedent) part of the rule. 3) Implication from the antecedent to the consequent (THEN part of the rules). 4) Aggregation of the consequents across the rules. 5) Defuzzification.

The crisp inputs are converted to linguistic variables in fuzzification based on membership function (MF). An MF is a curve that defines how the values of a fuzzy variable in a certain domain are mapped to a membership value μ (or degree of membership) between 0 and 1. A membership function can have different shapes. The simplest and most commonly used MF is the triangular-type, which can be symmetrical or asymmetrical in shape. Two MFs are built on the Gaussian distribution curve: a simple Gaussian curve and a two-sided composite of two different Gaussian distribution curves. The implication step helps to evaluate the consequent part of a rule. Mamdani is proposed, which is the most commonly used implication method. In this, the output is truncated at the value based on degree of membership to give the fuzzy output.

The control objectives of the qZS-CMI based grid-tie PV system are: 1) the distributed MPPT to ensure the maximum power extraction from each PV array; 2) the power injection to the grid at unity power factor with low harmonic distortion; 3) the same dc-link peak voltage for all qZS-HBI modules. The overall control scheme of Fig. 2 is proposed to fulfill these purposes

Total PV array voltage loop adjusts the sum of n PV array voltages tracking the sum of n PV array voltage references by using fuzzy logic controller (FLC). Each PV array voltage reference is generated independently from its MPPT control.

Grid-tie current loop ensures a sinusoidal grid-injected current in phase with the grid voltage. The total PV array voltage loop outputs the desired amplitude of grid-injected current. A Proportional + Resonant (PR) regulator [1] enforces the actual grid current to track the desired grid-injected reference. The current loop output's total modulation signal subtracts the modulation signal sum of the second, third, ..., and Kth qZS-HBI modules to get the first qZS-HBI module's modulation signal.

The separate n-1 PV array voltage loops regulate the other n-1 PV array voltages to achieve their own MPPT through the n-1 FLC's, such as FLC1 to FLCN, respectively. With the total PV array voltage loop control, the n PV arrays fulfill the distributed MPPT. In addition, the voltage feed forward control is used to generate each qZS-HBI module's modulation signal, which will reduce the regulators' burden, achieve the fast dynamic response, and minimize the grid voltage's impact on the grid-tie current.

In order to achieve the same dc-link voltage for all the modules, the dc-link peak voltage is adjusted in terms of its shoot-through duty ratio for each qZS-HBI module, as Fig. 2(b) shows. A proportional (P) regulator is employed in the inductor L_2 current loop to improve the dynamic response, and a fuzzy logic controller of the dc-link voltage loop ensures the dc-link peak voltage tracking the reference. Finally, the independent modulation signals V_{MK} and shoot through duty ratios D_K of the qZS-CMI, $K \in \{1, 2, 3, \dots, n\}$ are combined into the proposed multilevel SVM to achieve the desired purposes.

III .SYSTEM MODELING AND CONTROL

The modeling of the proposed system and its control are discussed in this section.

A. Grid - Tie current Loop

The k^{th} qZS-HBI module has following dynamic equation:

$$i_{L1k} = i_{PVk} - C_p \frac{dV_{PVk}}{dt} \quad (4)$$

where i_{L1k} the current of qZS inductor is L_1 , i_{PVk} is the K^{th} PV array's current, and C_p is the capacitance of PV array terminal capacitor.

The qZS-CMI based grid-tie PV system has

$$v_H = V_g + L_f \frac{di_s}{dt} + r_f i_s \quad (5)$$

Where V_g is the grid voltage, i_s is the grid-injected current, L_f is the filter inductance, r_f and is its parasitic resistance. The transfer function of the grid-injected current can be

$$G_f(s) = \frac{I_s(s)}{V_H(s) - V_g(s)} = \frac{1}{L_f(s) + r_f} \quad (6)$$

A PR regulator is employed to enforce the actual grid-injected current to track the desired reference

$$v_{mk} = v'_{mk} + v_g(s) G_{vfk}(s) \quad (7)$$

$$G_{vfk}(s) = \frac{1}{n G_{invk}(s)}$$

$$G_{invk}(s) = \frac{V_{Hk}(s)}{V_{mk}(s)} = V_{Dck} \quad (8)$$

where v'_{mk} is the regulated modulation signal from the separate voltage control of the Kth module, as Fig. 4 shows. From (7) and (8), we have

$$\begin{aligned} V_H(s) &= \sum_{K=1}^n v_{mk} G_{innvk}(s) \\ &= \sum_{k=1}^n v'_{mk} G_{invk}(s) + (s) G_{Vfk}(s) G_{invk}(s) \quad (9) \end{aligned}$$

At the dc-link peak voltage balance control, all dc-link peak voltages are the same. The n qZS-HBI modules have the same transfer function, and we assume

$$G_{invk}(s) = G_{inv}(s), k \in \{1; 2; \dots, n\} \quad (10)$$

Using 6-10, the grid injected current will be

$$I_s(s) = G_f(s) G_{inv}(s) \sum_{k=1}^n v'_{mk} \quad (11)$$

Then, the current loop can be simplified as shown in Fig. 4, and the open-loop transfer function can be obtained as

$$G_{io}(s) = \frac{I_s(s)}{v'_m(s)} = G_{inv}(s) G_f(s) = \frac{v^{dck}}{L_f(s) + r_f} \quad (12)$$

With the compensation of the PR regulator, the transfer function becomes

$$G_{icom}(s) = G_{PRi}(s) G_{io}(s) \quad (13)$$

$$G_{icom}(s) = \frac{V_{Dck}(K_{ip}s^2 + K_{ip}\omega_0^2 + K_{ip}\omega_0)}{L_f s^3 + r_f s^2 + s L_f \omega_0^2 + r_f \omega_0^2} \quad (14)$$

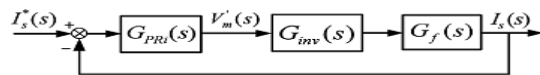


Fig.4. Simplified block diagram of the grid-current closed loop

B. PV Voltage Loop

The equation of the PV voltage can be written as

$$V_{PVk}(s) = \frac{1}{C_p(s)} [I_{PK}(s) - I_{L1k}(s)] \quad (15)$$

In addition, the output power of each qZS-HBI module equals to its input power in the non-shoot-through state, the kth qZS-HBI module has the power equation

$$\frac{\hat{I}_s \hat{V}_{Hk}}{2} = \hat{V}_{Dck} \bar{I}_{Dck} = v_{PVk} \bar{I}_{L1k_nsh} \quad (16)$$

where \bar{I}_{L1k_nsh} is the average current of inductor in nonshoot-through state. Using (1), \bar{I}_{L1k_nsh} can be solved as

$$\bar{I}_{L1k_nsh} = \frac{\hat{I}_s \hat{V}_{Hk}}{2 \hat{V}_{Dck} (1-2D_k)} \quad (17)$$

In the shoot-through state, the average current of inductor L_1 can be expressed as

$$\bar{I}_{L1k_nsh} = i_{PVk} = \bar{I}_{pvk} \quad (18)$$

$$\bar{I}_{L1k} = D_k \bar{I}_{L1k_sh} + (1 - D_k) \bar{I}_{L1k_nsh} \quad (19)$$

$$= D_k i_{pvk} + (1 - D_k) \bar{I}_{L1k_nsh} \quad (20)$$

Then, the control block diagrams of total and separate PV voltage loops can be obtained in Figs. 5 (a) and (b).

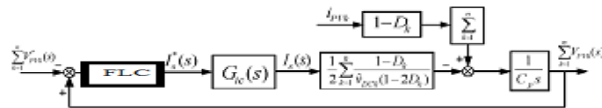


Fig.5(a). Block diagram of total PV voltage loop.



Fig.5 (b). Block diagram of separate PV voltage loop.

The closed-loop transfer function is

$$G_{vct}(s) = \frac{V_{PV} t(s)}{V_{PV}^* t(s)} = \frac{-G_{vcomt}(s)}{1 - G_{vcomt}(s)} \quad (21)$$

Similarly, from Fig. 5(b), the transfer function of the Kth qZS-HBI module's PV voltage loop, $k \in \{2,3,\dots,n\}$, is given as

$$G_{vck}(s) = \frac{V_{PVk}(s)}{V_{PVk}^*} = \frac{-G_{vcomk}(s)}{1 - G_{vcomk}(s)} \quad (22)$$

C.DC – Link Voltage Controller

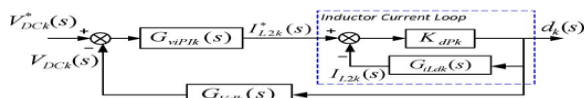


Fig.6. Block diagram of the Kth module's dc-link peak voltage control

The independent dc-link peak voltage control based on the inductor- L_2 current and the capacitor- C_1 voltage is performed for each qZS-HBI module, as Fig. 2(b) shows. From [1], the K^{th} qZS-HBI module's transfer functions from the shoot-through duty ratio to the dc-link peak voltage, $G_{vdck}(s)$, and from the shoot-through duty ratio to the inductor- L_2 current, $G_{idck}(s)$ can be obtained, respectively. With the employed fuzzy logic and proportional regulator at the coefficient K_{dtpk} for the inductor current loop, as in the block diagram of Fig. 6 shows, the closed-loop transfer function of inductor L_2 current and for dc link voltage loop can be obtained respectively as

$$G_{idck}(s) = \frac{d_k(s)}{I_{L2k}^*(s)} = \frac{K_{dtpk}}{1 + k_{dtpk} G_{ildk}(s)} \quad (23)$$

$$G_{Vdck}(s) = \frac{d_k(s)}{V_{Dck}^*} = \frac{G_{idck}(s)}{1 + G_{idck}(s) G_{VDk}(s)} \quad (24)$$

IV. PROPOSED MULTILEVEL SVM FOR QZS- MI

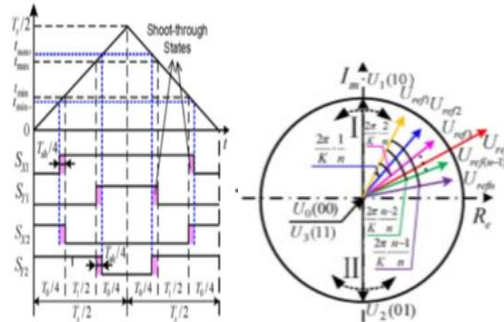


Fig 7: Proposed multilevel SVM for the single-phase qZS-CMI. (a) Switching pattern of one qZS-HBI module. (b) Synthesis of voltage vectors for the qZS-CMI.

The SVM for each qZS-HBI can be achieved by modifying the SVM technique for the traditional single-phase inverter [4]. Using the first qZS-HBI module of Fig. 2(a) as an example, the voltage vector reference U_{ref1} is created through the two U_1 vectors and U_0 by

$$U_{ref1} = U_1 \frac{T_1}{T_s} + U_0 \frac{T_0}{T_s} \quad (25)$$

where $T_s=1/f_c$ and f_c is the carrier frequency; the time interval T_1 is the duration of active vectors, and T_0 is the duration of traditional zero voltage space vectors. Thus, the switching times for the left and right bridge legs in traditional HBI are $\{t_L, t_R\} \in \{T_0/4, T_1/2+T_0\}$. However, the shoot-through states are required for the independent qZS-HBI module.

For this purpose, a delay of the switching times for upper switches or a lead of the switching times for lower switches are employed at the transition moments, as Fig. 7(a) shows. During each control cycle, the T_{sh} total time of shoot-through zero state is equally divided into four parts. The time intervals of $t_{min} \in \min \{t_L, t_R\}$ and $t_{max} \in \max \{t_L, t_R\}$ remain unchanged; $t_{min}^- = \{t_{min} - T_{sh}/4\}$ and $t_{max}^+ = \{t_{max} + T_{sh}/4\}$ are the modified times to generate the shoot-through states; S_{X1} and S_{Y1} are the switching control signals for the upper switches, S_{X2} and S_{Y2} are that for the lower switches, $\{X, Y\} \in \{L, R\}$. In this way, the shoot-through states are distributed into the qZS-HBI module.

To generate the step-like ac output voltage waveform from the qZS-CMI, a phase difference, $2\pi/(nK)$ in which K is the number of reference voltage vectors in each cycle, is employed between any two adjacent voltage vectors, as Fig. 7(b) shows. The total voltage vector U_{ref} is composed of n reference vectors $U_{ref1}, U_{ref2}, \dots, U_{refn}$ from the n qZS-HBI modules.

V. SIMULATION RESULTS

A seven-level qZS-CMI for grid-connected PV power system is simulated using Matlab Simulink model and the results are shown below:

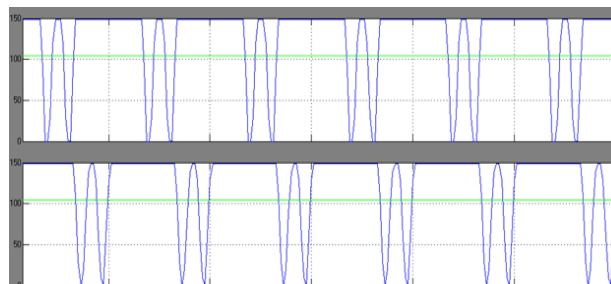


Fig8: Simulation results of DC link voltages with their shoot through periods (V_{DC1} & V_{pv1} ; V_{DC2} & V_{pv2})

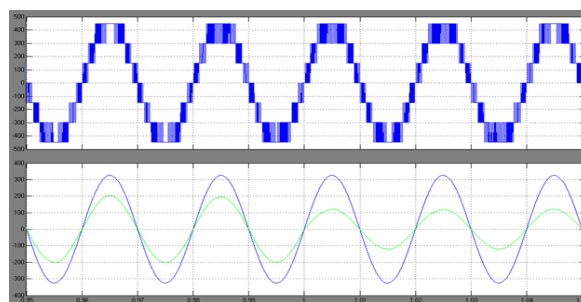


Fig9:(a).Seven level stepped output of the qZS-CMI .(b).Grid voltage and current,due to change in irradiation the value of current has been reduced..

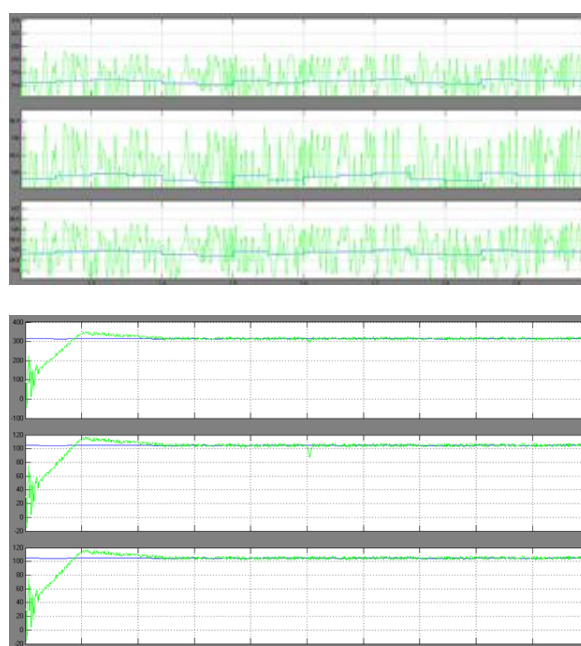


Fig 10: Simulation output of PV voltages with MPPT.

VI. CONCLUSION

The paper proposed a control method for qZS-CMI based single-phase grid-tie PV system. The grid-injected power was fulfilled at unity power factor, all qZS-HBI modules separately achieved their own maximum power points tracking even if some modules' PV panels are subjected to some change irradiation conditions. A multilevel SVM integrating with shoot through states was proposed to synthesize the staircase voltage waveform of the single-phase qZS-CMI. The simulation were carried out on the seven-level qZS-CMI which was tested and verified. In principle, the proposed system can work with the weak grid and can be extended for three phase grid connection.

REFERENCES

- [1] "An Effective Control Method for Quasi-Z-Source Cascade Multilevel Inverter-Based Grid-Tie Single-Phase Photovoltaic Power System" Yushan Liu, Student Member, IEEE, BaomingGe, Member, IEEE, Haitham Abu-Rub, Senior Member, IEEE, and Fang Z. Peng, Fellow, IEEE.
- [2] J. Chavarria, D. Biel, F. Guinjoan, C. Meza, and J. J. Negron, "Energy balance control of PV cascaded multilevel grid-connected inverters under level-shifted and phase-shifted PWMs," *IEEE Transactions on Industrial Electronics*, vol. 60, no. 1, pp. 98–111, Jan. 2013.
- [3] D. Sun, B. Ge, F. Z. Peng, H. Abu-Rub, D. Bi, and Y. liu, "A new grid-connected PV system based on cascaded H-bridge quasi-Z source inverter," in *Proc. IEEE Int. Symp. Ind. Electron.*, May 28–31, 2012, pp. 951–956.

- [4] J. I. Leon, S. Vazquez, J. A. Sanchez, R. Portillo, L. G. Franquelo, J.M.Carrasco, and Dominguez “Conventional space-vector modulation techniques versus the single-phase modulator for multilevel converters ,” *IEEE Trans. Ind. Electron.*, vol. 57, no. 7, pp. 2473–2482, Jul. 2010.
- [5] M. A. G. de Brito, L. Galotto, L. P. Sampaio, G. de Azevedo e Melo, and C. A. Canesin, “Evaluation of the main MPPT techniques for photovoltaic applications,” *IEEE Trans. Ind. Electron.*, vol. 60, no. 3, pp. 1156–1167, Mar. 2013.
- [6] H. Abu-Rub, A. Iqbal, Sk. Moin Ahmed, F. Z. Penz, Y. Li, and B. Ge, “Quasi-Z-source inverter-based photovoltaic generation system with maximum power tracking control using ANFIS,” *IEEE Trans. Sustain. Energy*, vol. 4, no. 1, pp. 11–20, Jan. 2013.
- [7] “Comparative Study of Proportional–Integral, Sliding Mode, and Fuzzy Logic Controllers for Power Converters “V. S. C. Raviraj and P. C. Sen, Fellow, IEEE